



Hydroclimate and bedrock permeability determine young water fractions in streamflow across the tropical Andes mountains and Amazon floodplain

5 Emily I. Burt¹, Daxs Herson Coayla Rimachi^{2,3}, Adan Julian Ccahuana Quispe², A. Joshua West¹

¹Zumberge Hall of Science 325C, 3651 Trousdale Pkwy, Los Angeles, California, USA 90089.

²Universidad Nacional San Antonio Abad del Cusco (UNSAAC), Cusco, Peru.

³Universidad Científica del Sur, Lima, Peru.

10

Correspondence to: Emily I. Burt, eburt@usc.edu

15

20

25



Abstract

The role of topography on water transit times and pathways through catchments is unclear, especially in
30 mountainous environments — yet these environments play central roles in global water, sediment, and
biogeochemical fluxes. Moreover, the vast majority of intensively monitored catchments are located in
northern latitudes. As a result, the interplay between water transit, topography and other landscape
characteristics is particularly underexplored in tropical environments. Here we present the results of a
multi-year hydrologic sampling campaign (twice-monthly and storm sampling) to quantify water transit in
35 seven small catchments ($< 3 \text{ km}^2$) across the transition from the Andes mountains to Amazon floodplain in
southern Peru. We use the stable isotope composition of water ($\delta^{18}\text{O}_{\text{H}_2\text{O}}$) to calculate the fraction of
streamflow comprised of recent precipitation (“young water fraction”) for each of the seven small
catchments. Mean unweighted young water fractions (F_{yw}) are 3–10 % in the Andes, 15–23 % at mid-
elevation and 3–4 % in the foreland floodplain. Weighting the F_{yw} calculation by volume of streamflow and
40 precipitation yield F_{yw} of 7–47 %. Across these catchments, topography does not exert a clear control on
water transit; instead stream F_{yw} is controlled by a combination of hydroclimate and bedrock permeability.
Mid-elevation sites are posited to have the highest F_{yw} due to less permeable bedrock, poorly developed
soils and more frequent and intense rainfall. The data presented here allow us to explore relationships
between topography, bedrock permeability, hydroclimate and stream baseflow F_{yw} — particularly
45 highlighting the role of bedrock permeability and hydroclimate in determining water transit times in a
tropical mountain setting.

50

55

60



1. Introduction

As water moves from rainfall to river runoff, it is stored in soil and rock for variable amounts of time. The length of time it takes for rainfall to exit a catchment in streams and rivers, known as the water transit time, exerts an important control on biogeochemical and ecohydrologic processes. While water is within a catchment, it reacts with soil and rock, acquiring solutes (Gibbs, 1970; Drever, 1988), and it interacts with ecosystems, sustaining photosynthesis and transpiration (Allen et al., 2019; Rempe and Dietrich, 2018). Water transit times also influence the availability of freshwater resources and the potential for environmental hazards such as flooding.

70

Mountainous regions play particularly important roles in the global water cycle, receiving outsized amounts of precipitation and acting as “water towers” that store and gradually release water for drier downstream areas (Barnett et al., 2005; Immerzeel et al., 2020; Meybeck et al., 2001; Viviroli et al., 2007). The impacts of climate change on the water cycle (Scanlon et al., 2018; Wilusz et al., 2017), especially diminished snowpack and warming across altitudinal gradients in mountainous regions, emphasize the importance of understanding water transit times in mountainous systems. Beyond serving as water towers, mountains have high erosion rates, exposing fresh mineral surfaces to chemical weathering processes that control the geological carbon cycle (Gaillardet et al., 1999; Hilton and West, 2020). Mineral weathering reactions in mountainous environments are modulated by a balance between water transit and mineral supply and reactivity (Ameli et al., 2017; Berner, 1978; Maher, 2010, 2011; West et al., 2005). Understanding the linkages between hydrology, erosion and the carbon cycle depends on quantifying water transit in mountainous environments. Finally, mountainous regions control the export of sediment and nutrients to rivers downstream, playing important roles in water quality and regional biogeochemistry.

75

Despite their global hydrological importance, much is not understood about water transit times in mountain systems. Global data suggest that streamflow in mountainous catchments carries less young water than in more gently sloping catchments (Jasechko, 2016; Lutz et al., 2018), potentially because of long water flow paths through fractured bedrock (e.g., Muñoz-Villers et al., 2016). Yet the relationships between topography and young water fractions are weak, and few studies have tested these ideas across the dramatic topographic gradients of major mountain ranges. Moreover, other studies have suggested complex relationships between topography and water transit times, with other factors including watershed organization and area, as well as bedrock permeability and subsurface structure, also playing important roles (Asano et al., 2002; McGlynn et al., 2003; McGuire et al., 2005; Tetzlaff, Seibert, McGuire, et al., 2009; Tetzlaff, Seibert, & Soulsby, 2009; Asano & Uchida, 2012; Hale et al., 2016; Hale & McDonnell,

85

90



95 2016; Xiao et al., 2021). Altogether, it remains unclear to what extent mountain regions affect fluid transit times, and for what reasons.

To address this problem, we collected a four-year time series (2016–2019) of approximately fortnightly stream and precipitation samples from seven small (< 3 km²) catchments in southern Peru. The study
100 catchments are within the Madre de Dios region in southern Peru, which includes the transition from the eastern Andes mountains (3472 m) to Amazon foreland floodplain (214 m; Fig. 1) and a gradient in catchment slopes from 37–3 °. We present a systematic evaluation of the movement and retention of water within these varied tropical landscapes, focusing on isotope-derived stream young water fractions. Because stable isotopes of precipitation vary with time, and the stable isotope composition of water is conservative
105 during transport through catchments, a comparison of time series of stable O or H isotopes in rainfall and stream water can be used to infer transit time (McGuire & McDonnell, 2006). The most general and robust interpretive framework uses isotope time series to calculate the stream young water fraction, which is the fraction of streamflow that fell as precipitation within the prior 2–3 months (Kirchner, 2016a, b). We build a stable isotope dataset and analyze the young water fractions across a range in topography (3472–214 m)
110 and slopes (37–3 °) rarely seen in other studies, allowing us novel insight into the effect of mountains on water transit. Moreover, we provide stable isotope constraints on water transit in tropical lowlands, where little information of this kind has been reported previously.

115 2. Data and methods

2.1 Study area and sampling design

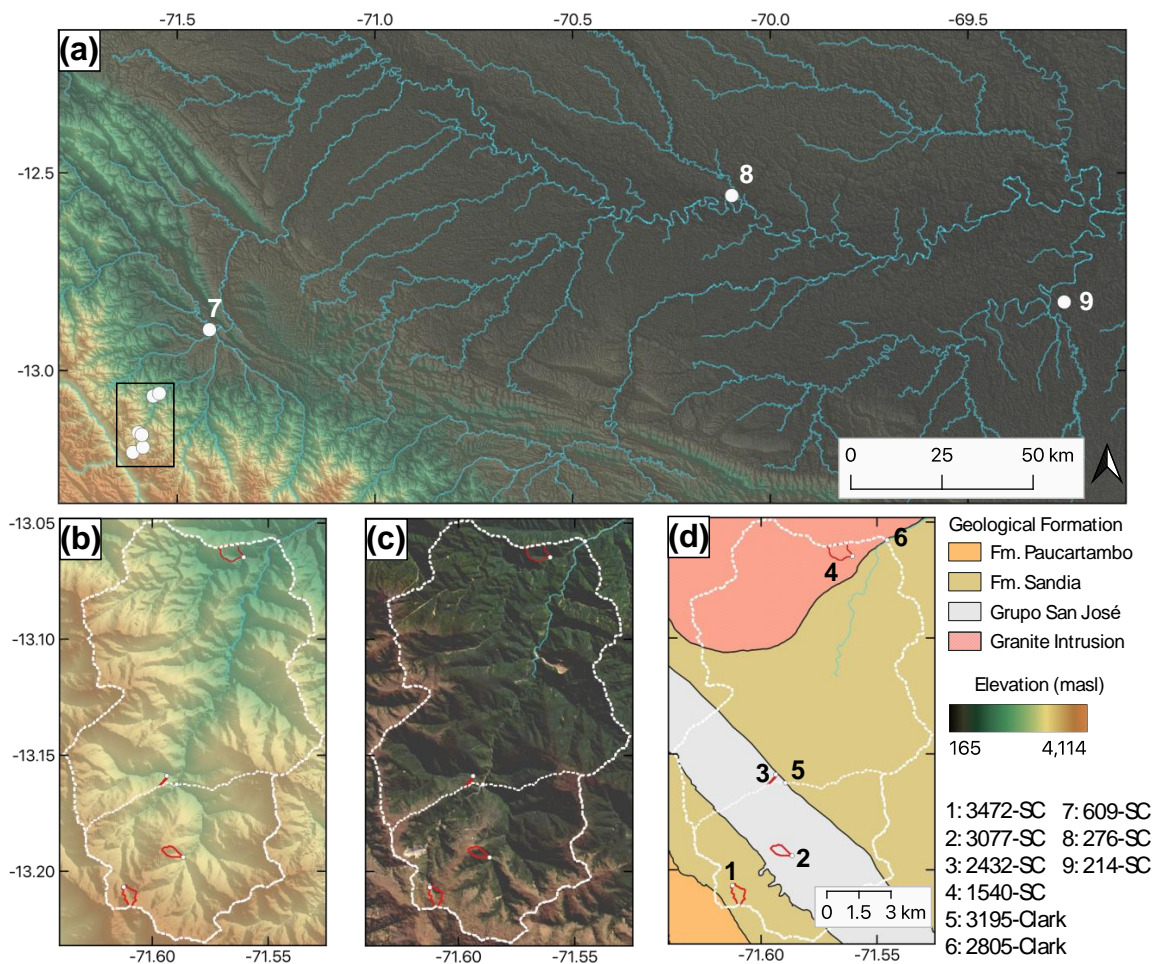
In this study, we carried out detailed hydrochemical monitoring at seven small (areas ranging from
120 0.03–3.00 km²) catchments spanning the transition from the eastern flank of the Andes Mountains to the Amazon foreland floodplain (Fig. 1; Table 1). The small catchments (SC) in this study are referred to by their sampling point elevation in meters, followed by “-SC”. Two small catchments (3472-SC and 3077-SC) are in the high Andes mountains, underlain by fractured shale bedrock, with mean slopes ranging from ~25–35 °. Two mid-elevation small catchments (2432-SC and 1540-SC) are in the similarly steep mid-
125 elevation Andes, with one (1540-SC) underlain by a granitic intrusion. One small catchment is situated in the foreland fold and thrust belt at the foothills of the Andes (609-SC), underlain by uplifted Andean sediments, with a mean slope of 20.8 °. Two of the small catchments are situated on fluvial terraces in the



foreland floodplain (276-SC and 214-SC), with the bedrock at these sites comprised of weathered
sediments from the Andes. These catchments have much lower slopes, averaging 3–4 °. We also consider
130 stable isotope data from two nested mesoscale catchments studied in Clark et al., 2014 (dashed white line in
Figure 1B-D). The catchments from Clark et al., 2014 are referred to by their mean elevation in meters,
followed by “-Clark”: 3195-Clark (mean slope 26 °; mean area 49 km²) and 2805-Clark (mean slope 28 °;
mean area 164 km²). Site 3195-Clark drains Andean shales and site 2805-Clark drains Andean shales and
the same granitic intrusion that underlies 1540-SC (Figure 1D).

135

The seven small streams were sampled approximately bi-weekly beginning in April 2016. In addition to
stream sampling, precipitation was collected at sites 3077-SC, 1540-SC, 609-SC, 276-SC and 214-SC. For
sites 3472-SC and 2432-SC we calculated approximate precipitation oxygen isotope values by linearly
interpolating between nearby precipitation samples collected at higher and lower elevations, supported by
140 the observation that in this region precipitation isotopes have a linear relationship with elevation (Ponton et
al., 2014). Precipitation was collected in a bucket left out between each sampling trip, with a layer of oil to
prevent evaporative loss. Point discharge was manually measured each time a sample was taken. For sites
3077-SC and 609-SC, continuous discharge was measured in 2019 and 2020 with WL16 Global Water
Level Loggers. Rainfall amount data are from tipping bucket and Vaisala rain gauges maintained by the
145 Andes Biodiversity and Ecosystem Research Group, a manual rain gauge maintained by the Los Amigos
Biological Station, and rain gauges operated by the Servicio Nacional de Meteorología e Hidrología del
Perú (SENAMHI).



150

Figure 1. (a) Digital Elevation Model (DEM, from ALOS 30m data) of the Andes mountains and Amazon floodplain in southern Peru. White circles indicate sampling locations. (b–d) show the area within the black rectangle in (a), with small catchments from this study delineated by solid red lines, and catchments from Clark et al., 2014 by dashed white lines. (b) shows elevation of Andean sites, (c) Landsat imagery, and (d) geology, using data from INGEMMET.

155

160



Sites, this study	Location	S	W	Area (km ²)	Mean slope (°)	Geology	Vegetation
3472-SC	Carretera Manu near Ajanaco	13.20617	71.61168	0.395	24.7	Sandia Fm. - shale	Puna
3077-SC	Wayqecha Biological Station	13.19255	71.58795	0.242	33.8	San José Group - shale	TMCF
2432-SC	Carretera Manu near Pillahuata	13.15969	71.59378	0.0287	29.5	San José Group - shale	TMCF
1540-SC	Carretera Manu near San Pedro	13.06454	71.56038	0.613	36.9	Granite Intrusion	UPRF
609-SC	Villa Carmen Biological Station	12.89614	71.41826	0.145	20.8	Paucartambo Fm.	Bamboo
276-SC	Los Amigos Biological Station	12.55884	70.09931	0.377	4.5	Fluvial terrace (Quaternary)	TRF
214-SC	Explorer's Inn Tambopata	12.82955	69.27132	3.00	3.2	Fluvial terrace (Quaternary)	TRF
Sites, existing dataset	Location	S	W	Area (km ²)	Mean slope (°)	Geology	Vegetation
3195-Clark	Kosñipata River at Wayqecha	13.16278	71.58917	49.8	27.5	Sandia Fm., San José Group	Puna, TMCF, UPRF
2805-Clark	Kosñipata River at San Pedro	13.06028	71.54444	165.2	29.9	Sandia Fm., San José Group, Granite Intrusion	Puna, TMCF, UPRF

Table 1. Characteristics of small catchments from this study and mesoscale catchments from Clark et al., 2014. TMCF = tropical montane cloud forest, UPRF = upper rainforest, TRF = tropical

165 **rainforest.**

170



2.2 Analytical techniques and data analysis

175 Samples were analyzed for stable isotopes of water ($\delta^{18}\text{O}$ and $\delta^2\text{H}$), with results reported here using
per mille notation relative to the Vienna Standard Mean Ocean Water standard. The stream oxygen or
hydrogen isotope composition is referred to as $\delta^{18}\text{O}_{\text{stream}}$ and $\delta\text{D}_{\text{stream}}$ and precipitation oxygen and hydrogen
isotope composition as $\delta^{18}\text{O}_{\text{precip}}$ and $\delta\text{D}_{\text{precip}}$. The analyses were carried out via two Los Gatos Research
Liquid Water Isotope Analyzers (LGR) (Caltech and Lawrence Berkeley National Lab) and a Picarro
L2130i Cavity Ring Down Spectrometer (Chapman University). The internal error of isotope
180 measurements on the Picarro was 0.1 ‰ or better for $\delta^{18}\text{O}$ and 2 ‰ or better for δD . On the LGR at
Lawrence Berkeley National Lab the internal error was 0.1 ‰ or better for $\delta^{18}\text{O}$ and 1 ‰ or better for δD .
On the LGR at Caltech the internal error was 0.3 ‰ or better for $\delta^{18}\text{O}$ and 1 ‰ or better for δD . Long-term
accuracy on certified isotope standards was within one standard deviation of the known isotopic values.

185 Young water fractions were calculated for each small catchment following Kirchner (2016a, 2016b).
Stream and precipitation oxygen isotope data were fit with Equation (1):

$$C(t) = a_s \times \cos(2\pi ft) + b_s \times \sin(2\pi ft) + k \quad (1)$$

where C is the concentration of a tracer in stream or precipitation, t is time, f is the frequency of the
interval, a and b are the cosine and sine coefficients and k is the vertical shift. The fit to stream and
190 precipitation isotope data was performed with and without stream discharge and rainfall amount weighting.
The young water fraction was then calculated using Equations (2-4), where:

$$\text{Amplitude, } \delta^{18}\text{O}_{\text{Stream}} = \sqrt{a_s^2 + b_s^2} \quad (2)$$

$$\text{Amplitude, } \delta^{18}\text{O}_{\text{Precipitation}} = \sqrt{a_p^2 + b_p^2} \quad (3)$$

$$\text{Young water fraction (\%)} = \text{Amplitude, } \delta^{18}\text{O}_{\text{Stream}} / \text{Amplitude, } \delta^{18}\text{O}_{\text{Precipitation}} \quad (4)$$

195

A Monte Carlo simulation was performed to assess the uncertainty associated with the young water fraction
calculations, using resampling with replacement to generate 10,000 stream and isotope datasets, and then
applying equations (1–4) to each dataset. In order to assess the differences in young water fraction
distributions between sites, a null dataset was generated using all of the stream and precipitation isotope
200 data across all of the sites, by subtracting each individual isotope value from the site-specific mean isotope
value. We then applied the same Monte Carlo resampling routine and equations (1–4) to the null dataset.
Stream baseflow indices were calculated for sites 3077-SC and 609-SC using the Matlab HydRun
hydrograph analysis package (Tang and Carey, 2017).

205



3. Results

3.1 Oxygen and hydrogen isotopes in streamflow and precipitation

The $\delta^{18}\text{O}_{\text{stream}}$ and $\delta^{18}\text{O}_{\text{precip}}$ values follow an orographic trend across the transition from high Andes
210 mountains to foothills (3472-SC to 609-SC), with the highest elevation streams showing the most isotopic
depletion (Fig. 2, 3b). Along this same mountain-to-foothill transition, $\delta^{18}\text{O}_{\text{precip}}$ and $\delta\text{D}_{\text{precip}}$ display a
marked seasonal cycle (amplitude $\delta^{18}\text{O}_{\text{precip}} \sim 4\text{--}5\text{‰}$) that is slightly greater in the Andes mountains than
the foothills or foreland floodplain (Table 2; Figs. 2b, 4c–d).

215

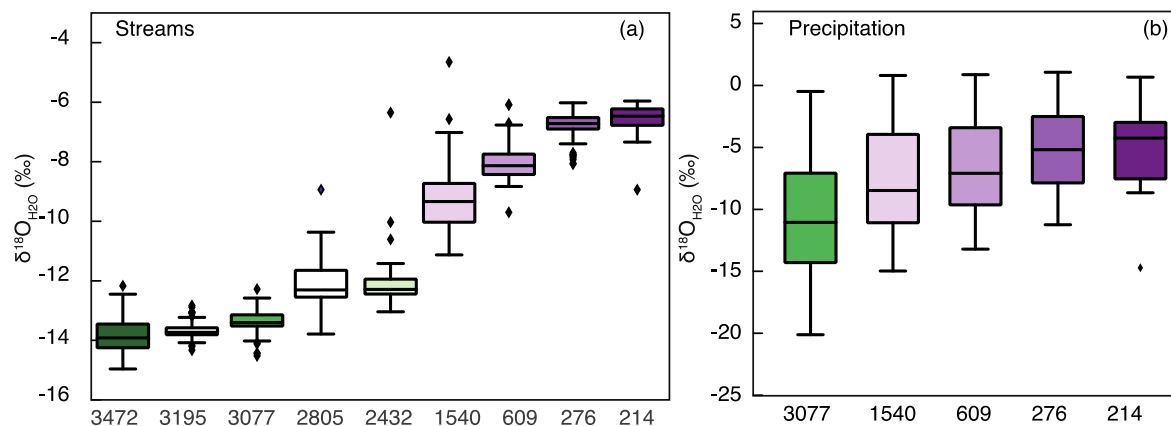


Figure 2. Boxplots of stream (a) and precipitation (b) $\delta^{18}\text{O}_{\text{H}_2\text{O}}$. Sites 3195 and 2805 are mesoscale catchments from Clark et al. (2014).

220

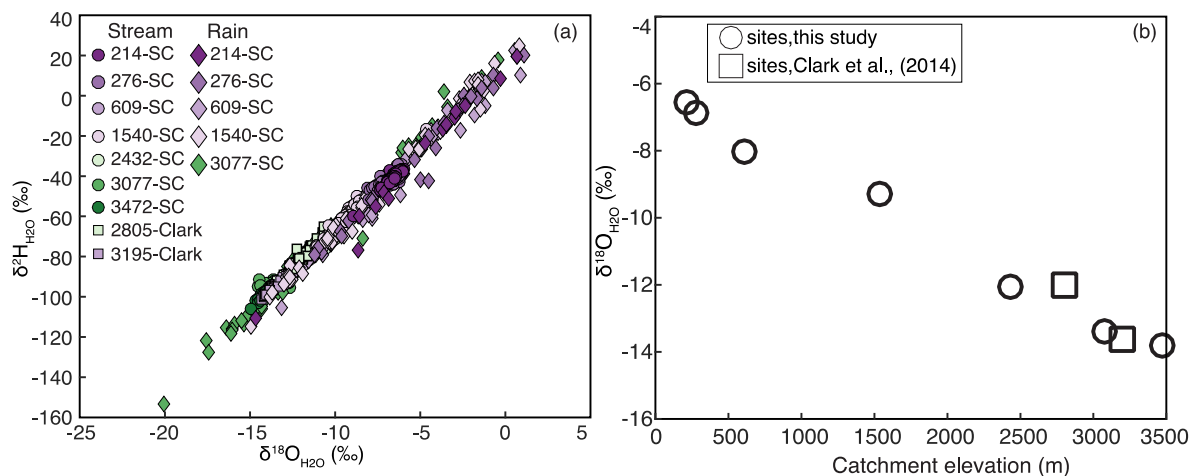
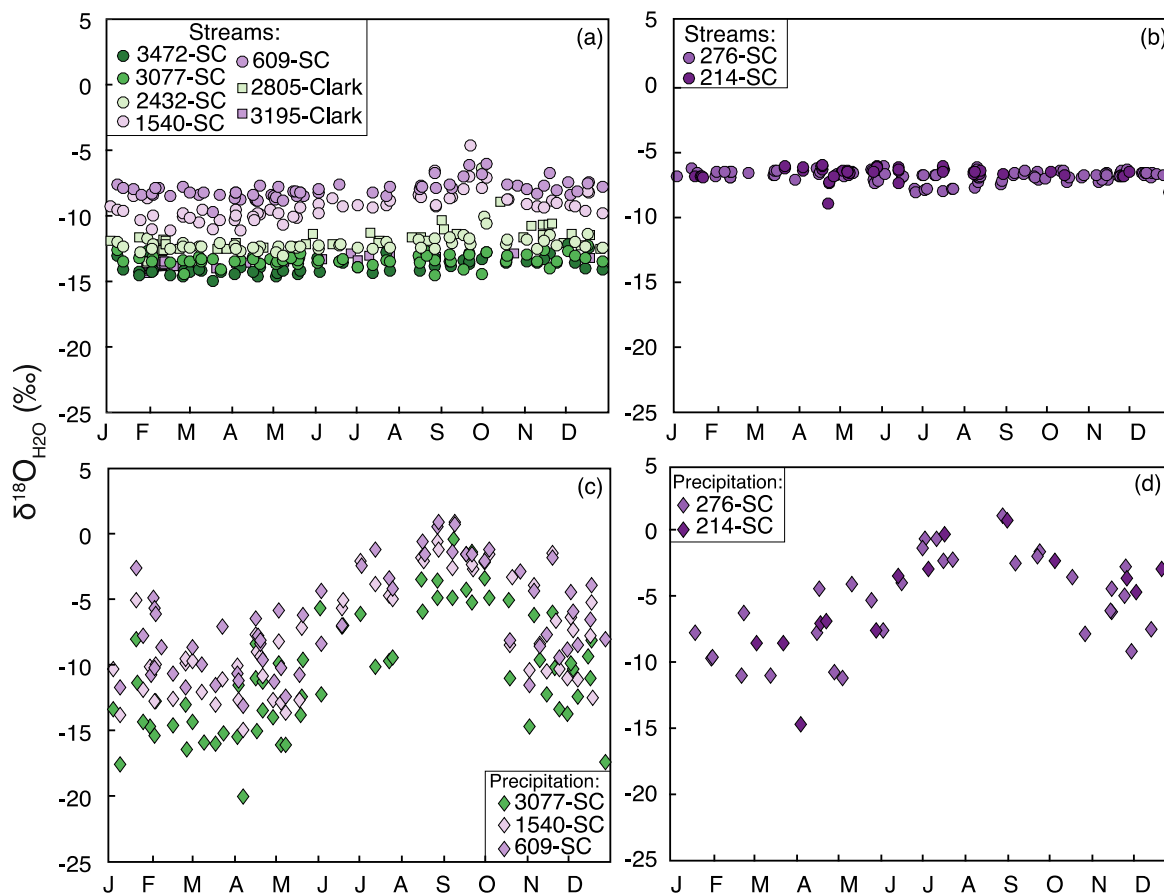


Figure 3. (a) $\delta^{18}\text{O}$ and δD of stream and precipitation. (b) mean $\delta^{18}\text{O}_{\text{stream}}$ as a function of catchment elevation at sampling point for the small catchments, and mean catchment elevation for the mesoscale catchments. Circles represent stream isotope data from this study, squares are mesoscale catchments from Clark et al. (2014) and diamonds are precipitation.

Relative to the $\delta^{18}\text{O}_{\text{precip}}$ inputs, $\delta^{18}\text{O}_{\text{stream}}$ values are damped. The degree of isotope dampening and
230 therefore the amplitude of the $\delta^{18}\text{O}_{\text{stream}}$ seasonal cycle varies between the small catchments situated from
mountain-to-foothill (Fig. 4a–b). The seasonal amplitude of $\delta^{18}\text{O}_{\text{stream}}$ values is smallest within the Andes
mountains (3472-SC, 3077-SC, 2432-SC) and foreland floodplain sites (276-SC and 214-SC) and highest
for the mid-elevation mountain (1540-SC) and mountain foothills sites (609-SC) (Fig. 2a, 4a–b). Of the
two mesoscale catchments, 3195-Clark has a smaller amplitude in $\delta^{18}\text{O}_{\text{stream}}$ than 2805-Clark. Dual isotope
235 space ($\delta^{18}\text{O}_{\text{H}_2\text{O}}$ and $\delta\text{D}_{\text{H}_2\text{O}}$) reveals no significant deviation from the local meteoric water line (Fig. 3a),
indicating no significant evaporative signal in the stream waters.



240 **Figure 4.** $\delta^{18}\text{O}_{\text{stream}}$ (a and b) and $\delta^{18}\text{O}_{\text{precip}}$ (c and d) for the duration of the study period (2016–2019),
plotted by day of year. $\delta^{18}\text{O}_{\text{stream}}$ from small catchments is denoted with circles, and the mesoscale
catchment data is denoted with squares. $\delta^{18}\text{O}_{\text{precip}}$ is denoted with diamonds. Panels (a) and (c) show
sites in the Andes and mountain foothills; panels (b) and (d) show the foreland floodplain sites.

245

250



255

Sites, this study	Location	<i>n</i> , stream samples	$\delta^{18}\text{O}_{\text{stream}}$, avg	Amplitude $\delta^{18}\text{O}_{\text{stream}}$	<i>n</i> , precip samples	$\delta^{18}\text{O}_{\text{precip}}$, avg.	Amplitude $\delta^{18}\text{O}_{\text{precip}}$
3472-SC	Mountain	55	-13.8	0.53	-	-	5.3
3077-SC	Mountain	63	-13.4	0.17	65	-10.5	5.1
2432-SC	Mountain	56	-12.0	0.57	-	-	5.2
1540-SC	Mid-elevation mountain	62	-9.3	1.13	60	-7.7	4.9
609-SC	Mountain foothills	66	-8.0	0.59	58	-6.6	4.0
276-SC	Foreland floodplain	95	-6.8	0.11	35	-5.3	4.2
214-SC	Foreland floodplain	28	-6.6	0.17	15	-5.0	4.9
<i>n samples total</i>		425			233		
Sites, published dataset	Location	<i>n</i> , stream samples	$\delta^{18}\text{O}_{\text{stream}}$, avg	Amplitude $\delta^{18}\text{O}_{\text{stream}}$	<i>n</i> , precip samples	$\delta^{18}\text{O}_{\text{precip}}$, avg.	Amplitude $\delta^{18}\text{O}_{\text{precip}}$
3195-Clark	Mountain	60	-13.7	0.42	-	5.29	-
2805-Clark	Mountain/mid-elevation mountain	62	-12.1	0.96	-	5.21	-
<i>n samples total</i>		122					

Table 2. Stream and precipitation stable water isotope data from this study and Clark et. al, 2014. ‘-’ indicates where samples were not collected. For sites without precipitation collection, $\delta^{18}\text{O}_{\text{precip}}$ was linearly interpolated by elevation from the nearest sites.

260

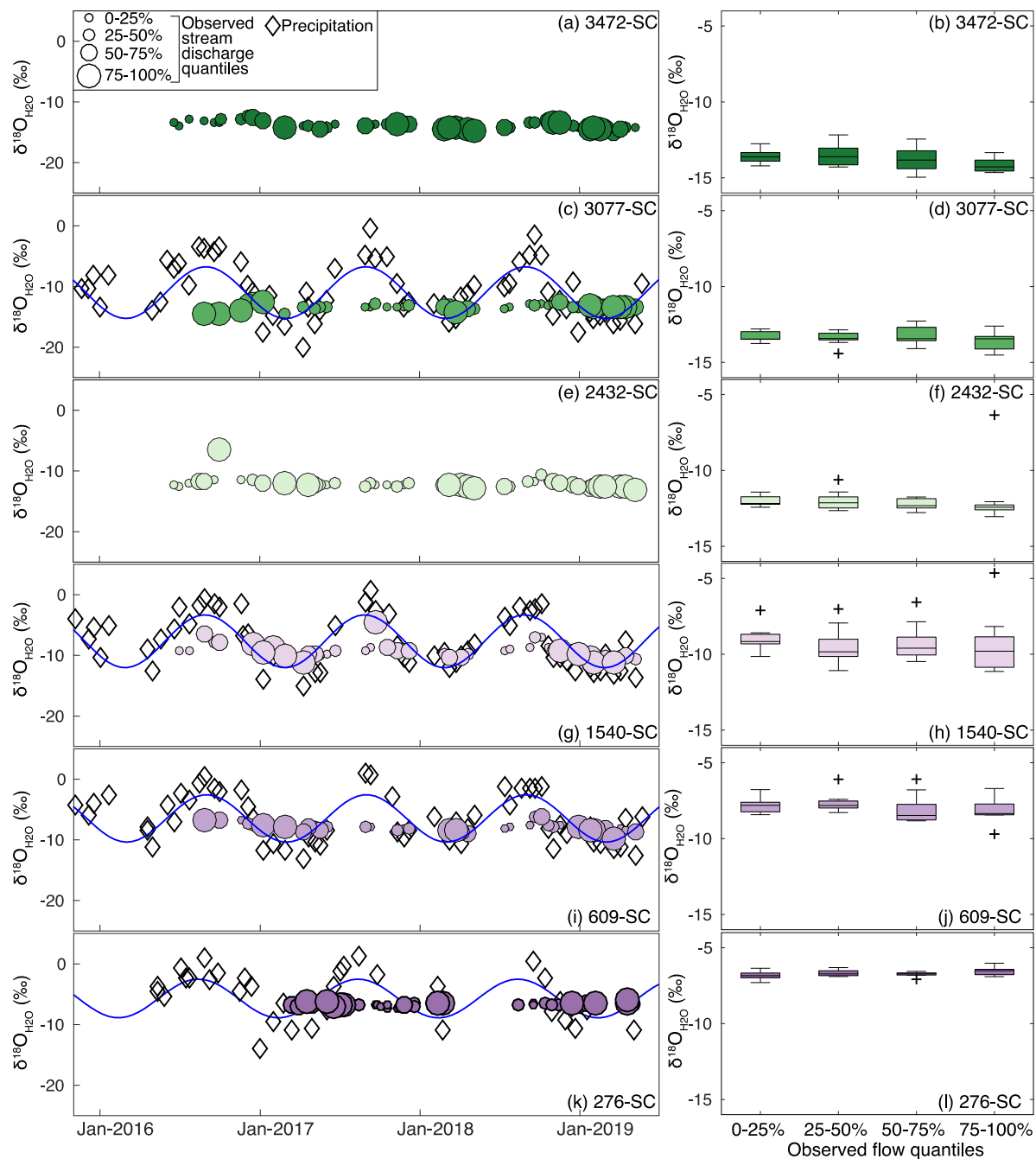
265



3.2 Young water fractions

270 Young water fractions (F_{yw}) vary between the catchments across the mountain-to-floodplain transition. Figure 7 shows calculated F_{yw} values for each catchment, with violin plots reflecting ranges generated using Monte Carlo simulation. 3472-SC, 3077-SC and 2432-SC have mean unweighted F_{yw} between 3 and 11 %. Mesoscale catchment 3195-Clark, draining approximately 50 km² of Andean shales, has a mean F_{yw} of 8 %, roughly averaging the F_{yw} seen in the three small Andean catchments. At mid-elevation, 1540-SC,
275 which drains granitic intrusions, has a mean unweighted F_{yw} of 23 %. The second mesoscale catchment, 2805-Clark, which drains a 165 km² area including Andean shales and granitic intrusions, has a mean unweighted F_{yw} of 18 %. 609-SC, in the foothills of the Andes and underlain by colluvium, has a mean unweighted F_{yw} of 15 %. On the foreland floodplain, 276-SC and 214-SC located on fluvial terraces, have mean unweighted F_{yw} of 3 and 4 %, respectively. For comparison, the null dataset, generated from a
280 compilation of isotope data from all sites, yields F_{yw} of 7 %. In addition to changes in the mean values across the Andes-Amazon gradient, the Monte Carlo distributions change, with wider distributions for the mid-elevation catchments and tighter distributions in the high Andes and Amazon lowland catchments.

285



290

Figure 5. $\delta^{18}\text{O}_{\text{stream}}$ (solid circles) and $\delta^{18}\text{O}_{\text{precip}}$ (open diamonds) from twice-monthly sampling campaigns in each small catchment. The size of the solid circles corresponds to the flow quantile that the $\delta^{18}\text{O}_{\text{stream}}$ is from. Data in (a–c) are from small catchments in the mountains, (d) is from the mid-elevation mountain small catchment, (e) is from the foothills small catchment and (f) is from the

295

foreland floodplain small catchment.



4. DISCUSSION

4.1 Hydroclimate and permeability controls on stream young water fractions

All else being equal, catchment topography is expected to control water transit times; steeper flow paths
300 should produce shorter transit times (e.g., following Darcy's Law), while greater relief may generate longer
flow paths and consequently longer transit times. Yet, despite much effort to demonstrate such effects, past
work has shown no systematic relationship between catchment topography and isotope-based young water
fractions, including in regional studies and across global compilations (e.g., Tetzlaff et al., 2009b).
Similarly, in our results, we find no simple relationship between catchment topography and F_{yw} across the
305 Amazon-Andes gradient studied here (Fig. 8). While unweighted F_{yw} is low (mean values <5 %) in both of
our lowland catchments (276-SC and 214-SC), the other catchments from mountain to foothills show a
wide range of unweighted F_{yw} , from 3–23 %, with no apparent relationship to either slope angle or flow
path length (Fig. 8a, b). There is, however, some coherent pattern in F_{yw} across these catchments that may
help to explain the decoupling of F_{yw} and topography at least across these sites, and perhaps more
310 generally.

Specifically, the small catchments in the high Andes Mountains (3472-SC, 3077-SC and 2432-SC) all have
low F_{yw} , with unweighted means between 3–10 % and relatively tight distributions, while the mid-elevation
small catchments show a much wider spread, tending toward much higher F_{yw} values (Fig. 7). The F_{yw}
315 values inferred from the mesoscale catchments studied by Clark et al. (2014) are consistent with the
patterns from the small catchments. The mesoscale catchment in the high Andes, underlain entirely by
shale bedrock, has a similar F_{yw} to that of the high elevation small catchments (unweighted mean value
<10%). In contrast, the mesoscale catchment that spans across the high- to mid-elevations (2805-Clark) has
an unweighted mean F_{yw} of 19%, consistent with a mixture of older water from upstream, high-
320 permeability shale-dominated portions of the study region and younger water from low-permeability
granitic areas. Overall, our data point to low and tightly distributed F_{yw} in the high mountains, but higher
and more broadly distributed F_{yw} in the mid-elevations.

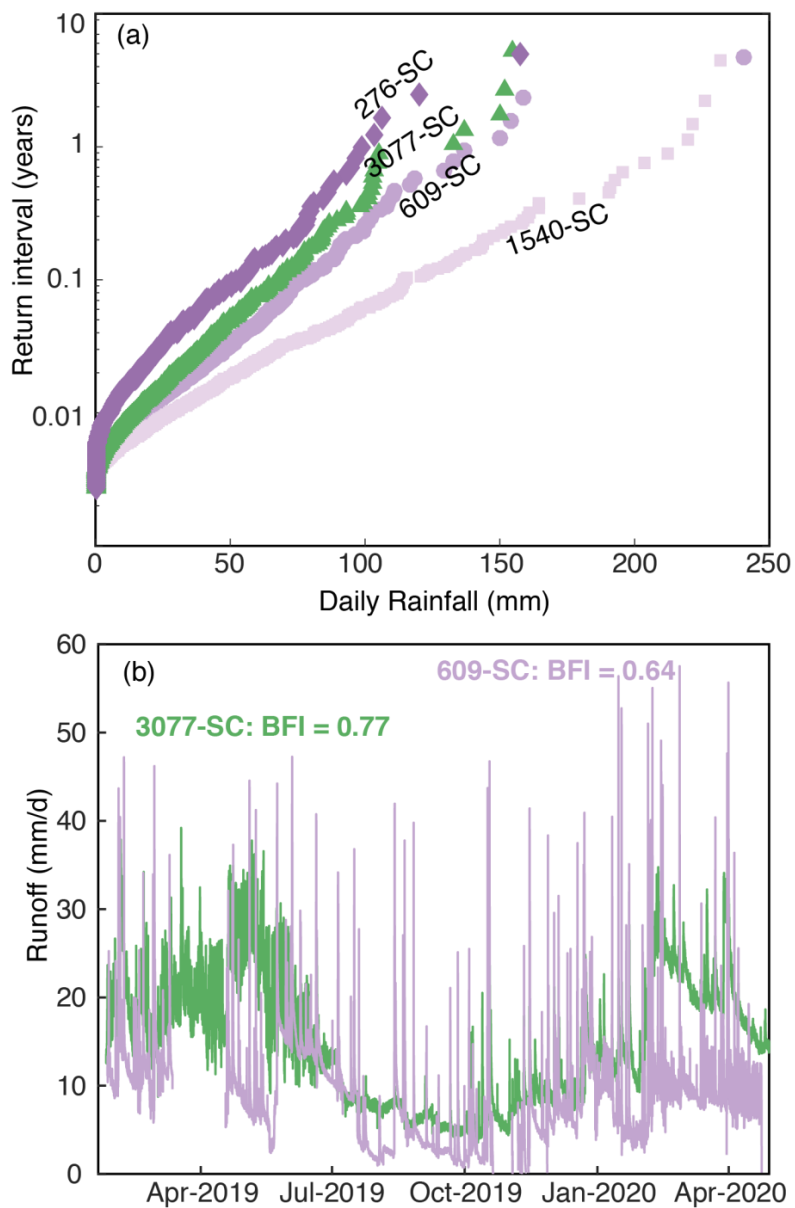
We attribute the low F_{yw} observed in the high mountain sites to high permeability of the fractured shale
325 bedrock. Fractures create conduits for fluid flow that can be magnified by dissolution of reactive minerals,
such as the sulfides that are relatively abundant in the Paleozoic shale underlying our Andes Mountains
catchments. Previous studies of stream hydrochemistry in the region have emphasized the importance of
sulfide mineral oxidation as a primary weathering process (Burt et al., 2021; Torres et al., 2016), and pyrite



oxidation is known to generate porosity and permeability in shale bedrock (Gu et al., 2020). In our
330 conceptual model of water transit, the combination of pore-scale chemical weathering and regional stresses
create a fractured subsurface that is conducive to long fluid flow paths, leading to overall low young water
fractions in Andean streams.

The mid-elevation catchments differ in two respects that we think can explain the distinct transit times
335 inferred for these streams. The increased spread in estimated F_{yw} for the catchments between 3000 and
500m coincides with a shift to a flashier hydroclimate, with more rainfall events of higher magnitude at the
mid-elevations compared to either the high Andes or the Amazon lowlands (Fig. 6a; also see Clark et al.,
2016). Correspondingly, the stream hydrograph at 609-SC is much flashier than at 3077-SC (Fig. 6b; these
are the two catchments with a semi-continuous discharge record). A comparison of stream baseflow indices
340 for sites 3077-SC and 609-SC shows a higher baseflow index for site 3077-SC (BFI = 0.77) and lower
baseflow index for site 609-SC (BFI = 0.64). We interpret the first-order shift in F_{yw} values from the high
Andes (where baseflow indices are high) to the mid-elevations (where baseflow indices are lower) as being
related to this change towards a stormier climate, suggesting a primary role for hydroclimate forcing in
determining transit times in these mountainous catchments. An important role for precipitation and
345 discharge regimes has emerged from other recent transit time studies focused on single catchments with
higher temporal resolution data collection (Gallart et al., 2020; von Freyberg et al., 2018; Stockinger et al.,
2016). Although we see some slight variability in the amplitude of $\delta^{18}O_{stream}$ as a function of discharge in
our results (Fig. 5), we lack data across the range of discharge that would be needed for robust quantitative
analysis of this effect. Higher frequency sampling across gradients such as those in the Andes, though
350 daunting given the logistical challenges of this environment, would be an interesting target for future work.

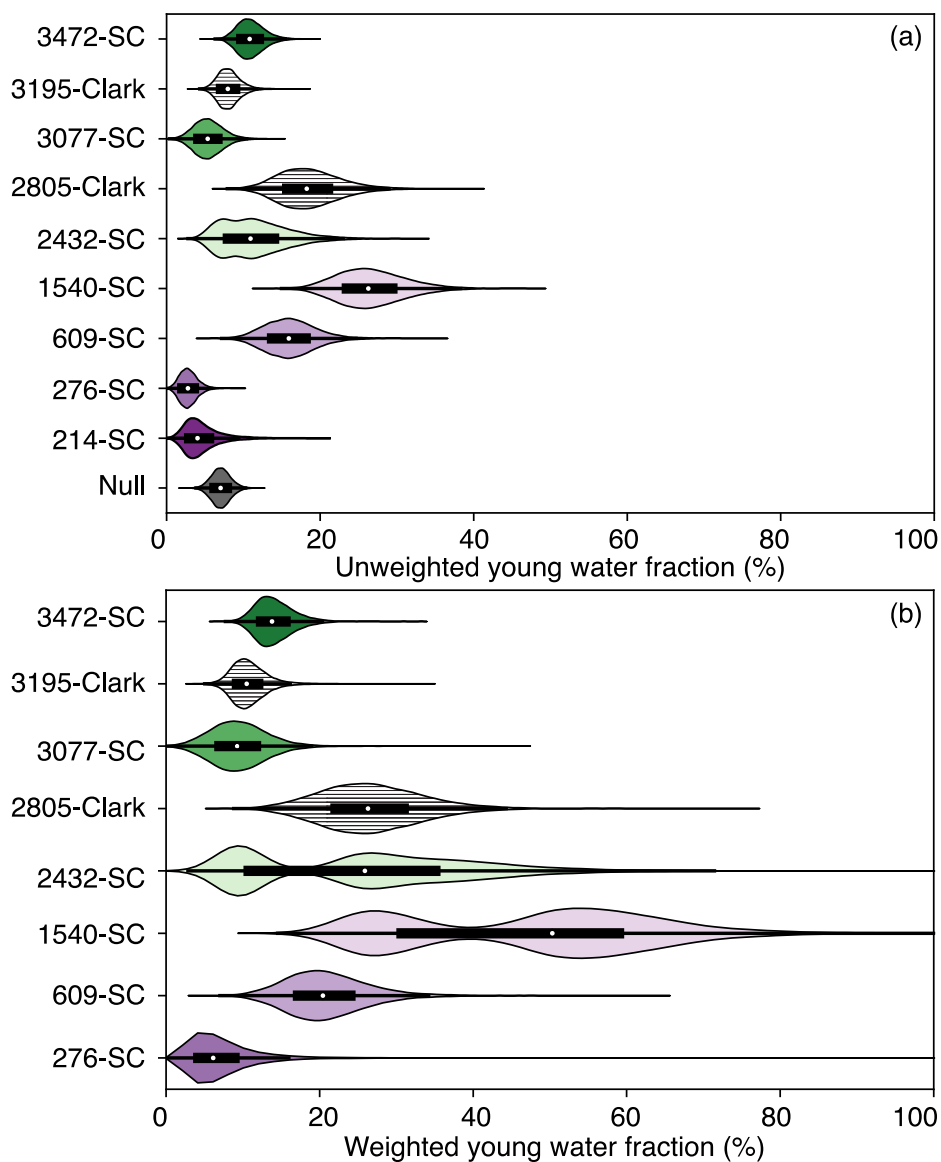
Superimposed on the overall differences that characterize the mid-elevation catchments, the F_{yw} in 1540-SC
stands out as especially high (Fig. 8; mean F_{yw} estimate >50% when amount-weighted). Unlike the other
catchments in our study that are characterized by sedimentary bedrock, this catchment is underlain by a
355 granitic intrusion (Clark et al., 2014). We attribute the especially high F_{yw} in this part of the study region to
the low permeability of this granite bedrock, which prevents water from infiltrating deeply and leads to
rapid, surficial flow paths over the steep topography. Altogether, then, we interpret the highly variable
transit times across the Andean catchments as being related principally to a combination of hydroclimate
and bedrock permeability, with these factors outweighing the influence of catchment topography.



360

Figure 6. (a) Precipitation return interval for rain gauges near sites 3077-SC, 1540-SC, 609-SC and 276-SC. (b) Stream runoff records for sites 3077-SC and 609-SC, showing baseflow indices for both sites.

365



370

Figure 7. Unweighted (a) and weighted (b) stream young water fractions for all catchments and a null dataset. 3195-Clark and 2805-Clark are the mesoscale catchments from Clark et al., 2014.

375



4.2 Implications for the role of mountains in modulating water, erosional, and biogeochemical fluxes.

380 The role of mountains as water towers, and particularly the response of these freshwater resources to
climate change, depends in part on water transit times through mountain catchments. In revealing the
importance of hydroclimate for transit times, our results suggest that shifting precipitation regimes may be
important in determining not just how much precipitation falls over mountain regions (or indeed the
balance of snow and rain), but also the fate of precipitation as it makes its way through mountain
385 catchments. If our spatial comparison of catchments across the Andes-Amazon region translates to
temporal trends, then a flashier rainfall regime in the future might be expected to produce a wider range of
transit times including higher young water fractions in streams draining mountainous terrain. In this sense,
our results are consistent with recent studies suggesting that catchments can amplify rainfall variability
(Müller Schmied et al., 2020). The implications for downstream flooding and the buffering of droughts
390 may warrant further consideration.

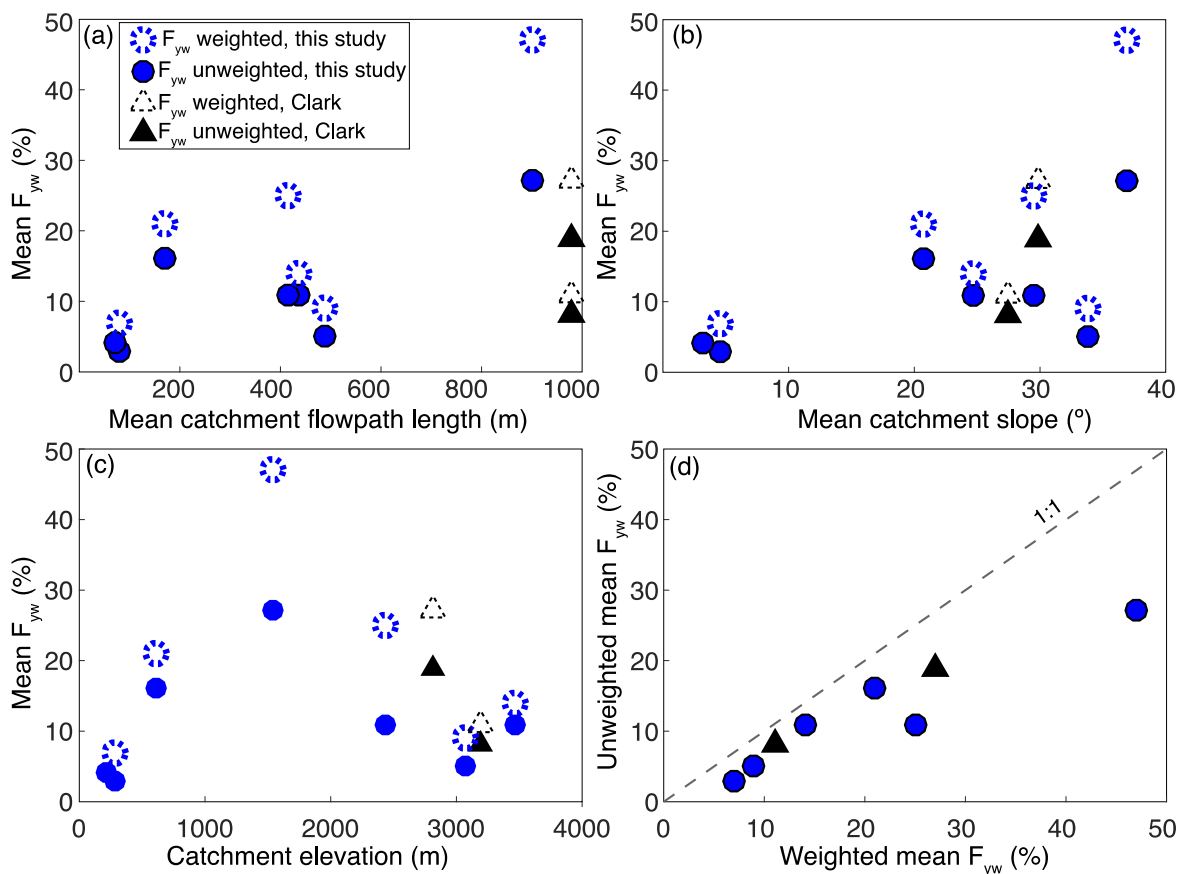
The hydrology of mountainous catchments may play important geological roles, too. River discharge, and
particularly discharge variability, exerts a primary control on erosion (e.g., Tucker and Bras, 2000). Longer
transit times may dampen the relationship between precipitation variability and the river incision that drives
395 mountain erosion; systematic relationships between topography and water transit times could therefore
either dampen or amplify erosional efficiency of a given precipitation regime. Catchment hydrology has
also been invoked as central to the role of mountain building in the global carbon cycle over geologic
timescales (Maher and Chamberlain, 2014). This argument depends on both the exposure of fresh minerals
for chemical weathering by rapid erosion, as well as systematic changes in hydrologic flow paths
400 associated with mountain building. However the mountainous sites within this study display a wide range
of values in F_{yw} (from ~3–23 %; Figure 8), with no systematic relationship between topography and F_{yw} .
Although a global compilation of stream F_{yw} shows a general negative correlation between topographic
relief and F_{yw} (Jasechko et al., 2016), that relationship is notably weak — and the F_{yw} from the small
catchments studied here emphasize how other environmental factors (hydroclimate, catchment architecture)
405 play important roles in determining the F_{yw} of streamflow. Moreover, when comparing across the high
Andes and Amazon lowlands, there is remarkably little difference in F_{yw} despite dramatic differences in
topography: catchments with average slope angles of ~5° and ~35° have similar F_{yw} ~5 %. This result
argues against a systematic shift in water transit times associated with mountain building, but rather a
variable response modulated by climatic and geologic factors — although our results do point to a wider
410 range in F_{yw} associated with mountains than lowlands, at least for the tropical setting of the Andes-Amazon
system.



While our results, and especially the F_{yw} of lowland catchments, may be specific to the Andes-Amazon setting, we expect the hydroclimatic and geological effects that we document here to be more generally
415 relevant in other mountainous regions, too. Orographic controls on precipitation tend to force the highest precipitation, as well as the most intense rainfall, along mountain fronts and at mid-elevations. In addition to the Andes, similar patterns have been shown in the Himalaya (Bookhagen and Burbank, 2006) and the European Alps (Napoli et al., 2019) and models predict complex spatial patterns of orographic precipitation that depend on several factors including climatic variables (e.g., (Barros and Lettenmaier, 1994; Roe and
420 Baker, 2006)The dependence of catchment transit times on hydroclimate, as we find in the Andes and as reported in other recent work (von Freyberg et al., 2018; Gallart et al., 2020), suggests that orographic effects on rainfall regime may be a primary determinant of hydrologic processes in major mountain ranges. Similarly, we expect fractured bedrock, and associated high permeability, to be generally characteristic of mountain systems as seen in our work and other studies (e.g., Muñoz-Villers et al., 2016; Moon et al.,
425 2017), though our results also highlight how the geological complexity of mountains – such as the presence of a granitic intrusion in our study area of the Andes – can introduce heterogeneity. Full understanding of the role of mountainous regions in water, sediment, and geochemical cycles will depend on evaluating the role of these multiple factors in determining hydrological behavior.

430

435



440

445

450

455

Figure 8. Circles represent small catchments from this study, triangles represent mesoscale catchments from Clark et al. (2014). In panels (a-c), dashed circles and triangles indicate volume weighted young water fractions; solid circles and triangles are unweighted young water fractions. (a) shows F_{yw} as a function of mean catchment flow path length, (b) shows F_{yw} as a function of mean catchment slope, (c) shows F_{yw} as a function of catchment elevation at sampling point for the small catchments, and mean catchment elevation for the mesoscale catchments. (d) Compares weighted mean F_{yw} to unweighted mean F_{yw} .



5. Conclusions

We collected stream and precipitation samples for analysis of O and H stable isotope ratios in rainfall and stream water at seven streams and four rainfall stations spanning the Andes-Amazon gradient over a period of four years. Samples were collected approximately twice monthly for most sites. The stream young water
460 fraction varied significantly between sites. Highest elevation sites 3472-SC, 3077-SC and 2432-SC displayed young water fractions between 3–10 %. Mid-elevation small catchments (1540-SC and 609-SC) displayed the higher young water fractions of 15–23 %. Catchments in the foreland floodplain had low young water fractions, ranging from 3–4 %.

465 We suggest that the low young water fractions observed in Andean catchments are a result of long flow paths in fractured shale. High young water fractions observed at mid-elevation sites result from a combination of a stormier climate, and in the case of 1540-SC, granitic bedrock with poorly developed soils and low permeability, meaning that water moves through the catchment faster. In the lowlands, low permeability clay terraces and low relief together generate low young water fractions. Thus a combination
470 of topography, climate, and bedrock properties conspire to determine water transit in this setting. Our results emphasize the complexity of the role of mountainous regions in the hydrological cycle and potentially help to explain why it has been difficult to identify a simple topographic control on young water fractions at the global scale. Accounting for the multiple factors that control water transit will be important for fully understanding the role of mountain water towers in water, sediment, and carbon fluxes.

475

480

485



Acknowledgements

490

This work was funded by NSF award EAR-1455352 to AJW. We thank the Andes Biodiversity and Ecosystem Research Group (ABERG) for field support and access to rainfall data. ABERG rainfall data were collected with support of NSF DEB LTREB 1754647 to Miles Silman. We thank Alex Sessions and Fenfang Wu at Caltech, Markus Bill at Lawrence Berkeley National Lab and Fernando Silva at Chapman
495 University for support with the stable isotope measurements. We thank Greg Goldsmith for support with stable isotope measurements and for helpful discussions. We thank Abra Atwood and Julien Emile-Geay for helpful discussions with respect to data analysis.

Code/Data availability

500

Stream and precipitation water isotope data are provided as a table. The Matlab code for young water fraction analysis and Monte Carlo simulation is available from E. Burt upon request.

Author contribution

505

EB and AJW designed the study with input from DHCR and AJCQ. EB, DHCR and AJCQ carried out the hydrochemical monitoring. EB analyzed the samples and did the data analysis with input from AJW. EB and AJW wrote the manuscript.

Competing interests

The authors declare no competing interests.

510

515

520



References

- 525 Allen, S. T., Kirchner, J. W., Braun, S., Siegwolf, R. T. W., and Goldsmith, G. R.: Seasonal origins of soil water used by trees, *Hydrol. Earth Syst. Sci.*, 23, 1199–1210, <https://doi.org/10.5194/hess-23-1199-2019>, 2019.
- Ameli, A. A., Beven, K., Erlandsson, M., Creed, I. F., McDonnell, J. J., and Bishop, K.: Primary weathering rates, water transit times, and concentration-discharge relations: A theoretical analysis for the critical zone: WEATHERING RATE, PERMEABILITY, STREAM C-Q, *Water Resour. Res.*, 53, 942–960, <https://doi.org/10.1002/2016WR019448>, 2017.
- 530 Asano, Y., Uchida, T., and Ohte, N.: Residence times and flow paths of water in steep unchannelled catchments, Tanakami, Japan, *J. Hydrol.*, 20, 2002.
- Barnett, T. P., Adam, J. C., and Lettenmaier, D. P.: Potential impacts of a warming climate on water availability in snow-dominated regions, *Nature*, 438, 303–309, <https://doi.org/10.1038/nature04141>, 2005.
- 535 Barros, A. P. and Lettenmaier, D. P.: Dynamic modeling of orographically induced precipitation, *Rev. Geophys.*, 32, 265, <https://doi.org/10.1029/94RG00625>, 1994.
- Berner, R. A.: Rate control of mineral dissolution under Earth surface conditions, *Am. J. Sci.*, 278, 1235–1252, <https://doi.org/10.2475/ajs.278.9.1235>, 1978.
- 540 Bookhagen, B. and Burbank, D. W.: Topography, relief, and TRMM-derived rainfall variations along the Himalaya, *Geophys. Res. Lett.*, 33, L08405, <https://doi.org/10.1029/2006GL026037>, 2006.
- Burt, E. I., Bill, M., Conrad, M. E., Quispe, A. J. C., Christensen, J. N., Hilton, R. G., Dellinger, M., and West, A. J.: Conservative transport of dissolved sulfate across the Rio Madre de Dios floodplain in Peru, *Geology*, <https://doi.org/10.1130/G48997.1>, 2021.
- 545 Clark, K. E., Torres, M. A., West, A. J., Hilton, R. G., New, M., Horwath, A. B., Fisher, J. B., Rapp, J. M., Robles Caceres, A., and Malhi, Y.: The hydrological regime of a forested tropical Andean catchment, *Hydrol. Earth Syst. Sci.*, 18, 5377–5397, <https://doi.org/10.5194/hess-18-5377-2014>, 2014.
- Clark, K. E., West, A. J., Hilton, R. G., Asner, G. P., Quesada, C. A., Silman, M. R., Saatchi, S. S., Farfan-Rios, W., Martin, R. E., Horwath, A. B., Halladay, K., New, M., and Malhi, Y.: Storm-triggered landslides in the Peruvian Andes and implications for topography, carbon cycles, and biodiversity, *Earth Surf. Dyn.*, 4, 47–70, <https://doi.org/10.5194/esurf-4-47-2016>, 2016.
- 550 Drever, J. I.: *The geochemistry of natural waters*, 2nd ed., Prentice Hall, Englewood Cliffs, N.J., 437 pp., 1988.
- von Freyberg, J., Allen, S. T., Seeger, S., Weiler, M., and Kirchner, J. W.: Sensitivity of young water fractions to hydro-climatic forcing and landscape properties across 22 Swiss catchments, *Hydrol. Earth Syst. Sci.*, 22, 3841–3861, <https://doi.org/10.5194/hess-22-3841-2018>, 2018.
- Gaillardet, J., Dupré, B., Louvat, P., and Allègre, C. J.: Global silicate weathering and CO₂ consumption rates deduced from the chemistry of large rivers, *Chem. Geol.*, 159, 3–30, [https://doi.org/10.1016/S0009-2541\(99\)00031-5](https://doi.org/10.1016/S0009-2541(99)00031-5), 1999.



- 560 Gallart, F., Valiente, M., Llorens, P., Cayuela, C., Sprenger, M., and Latron, J.: Investigating young water fractions in a small Mediterranean mountain catchment: Both precipitation forcing and sampling frequency matter, *Hydrol. Process.*, 34, 3618–3634, <https://doi.org/10.1002/hyp.13806>, 2020.
- Gibbs, R. J.: Mechanisms Controlling World Water Chemistry, *Science*, 170, 1088–1090, <https://doi.org/10.1126/science.170.3962.1088>, 1970.
- 565 Gu, X., Rempe, D. M., Dietrich, W. E., West, A. J., Lin, T.-C., Jin, L., and Brantley, S. L.: Chemical reactions, porosity, and microfracturing in shale during weathering: The effect of erosion rate, *Geochim. Cosmochim. Acta*, 269, 63–100, <https://doi.org/10.1016/j.gca.2019.09.044>, 2020.
- Hilton, R. G. and West, A. J.: Mountains, erosion and the carbon cycle, *Nat. Rev. Earth Environ.*, 1, 16, <https://doi.org/10.1038/s43017-020-0058-6>, 2020.
- 570 Immerzeel, W. W., Lutz, A. F., Andrade, M., Bahl, A., Biemans, H., Bolch, T., Hyde, S., Brumby, S., Davies, B. J., Elmore, A. C., Emmer, A., Feng, M., Fernández, A., Haritashya, U., Kargel, J. S., Koppes, M., Kraaijenbrink, P. D. A., Kulkarni, A. V., Mayewski, P. A., Nepal, S., Pacheco, P., Painter, T. H., Pellicciotti, F., Rajaram, H., Rupper, S., Sinisalo, A., Shrestha, A. B., Viviroli, D., Wada, Y., Xiao, C., Yao, T., and Baillie, J. E. M.: Importance and vulnerability of the world's water towers, *Nature*, 577, 364–369, <https://doi.org/10.1038/s41586-019-1822-y>, 2020.
- Jasechko, S.: Partitioning young and old groundwater with geochemical tracers, *Chem. Geol.*, 427, 35–42, <https://doi.org/10.1016/j.chemgeo.2016.02.012>, 2016.
- Jasechko, S., Kirchner, J. W., Welker, J. M., and McDonnell, J. J.: Substantial proportion of global streamflow less than three months old, *Nat. Geosci.*, 9, 126–129, <https://doi.org/10.1038/ngeo2636>, 2016.
- 580 Kirchner, J. W.: Aggregation in environmental systems – Part 1: Seasonal tracer cycles quantify young water fractions, but not mean transit times, in spatially heterogeneous catchments, *Hydrol. Earth Syst. Sci.*, 20, 279–297, <https://doi.org/10.5194/hess-20-279-2016>, 2016a.
- Kirchner, J. W.: Aggregation in environmental systems – Part 2: Catchment mean transit times and young water fractions under hydrologic nonstationarity, *Hydrol. Earth Syst. Sci.*, 20, 299–328, <https://doi.org/10.5194/hess-20-299-2016>, 2016b.
- 585 Lutz, S. R., Krieg, R., Müller, C., Zink, M., Knöller, K., Samaniego, L., and Merz, R.: Spatial Patterns of Water Age: Using Young Water Fractions to Improve the Characterization of Transit Times in Contrasting Catchments, *Water Resour. Res.*, 54, 4767–4784, <https://doi.org/10.1029/2017WR022216>, 2018.
- Maher, K.: The dependence of chemical weathering rates on fluid residence time, *Earth Planet. Sci. Lett.*, 294, 101–110, <https://doi.org/10.1016/j.epsl.2010.03.010>, 2010.
- Maher, K.: The role of fluid residence time and topographic scales in determining chemical fluxes from landscapes, *Earth Planet. Sci. Lett.*, 312, 48–58, <https://doi.org/10.1016/j.epsl.2011.09.040>, 2011.
- Maher, K. and Chamberlain, C. P.: Hydrologic Regulation of Chemical Weathering and the Geologic Carbon Cycle, *Science*, 343, 1502–1504, <https://doi.org/10.1126/science.1250770>, 2014.
- 595 McGlynn, B., McDonnell, J., Stewart, M., and Seibert, J.: On the relationships between catchment scale and streamwater mean residence time, *Hydrol. Process.*, 17, 175–181, <https://doi.org/10.1002/hyp.5085>, 2003.



- McGuire, K. J. and McDonnell, J. J.: A review and evaluation of catchment transit time modeling, *J. Hydrol.*, 330, 543–563, <https://doi.org/10.1016/j.jhydrol.2006.04.020>, 2006.
- 600 McGuire, K. J., McDonnell, J. J., Weiler, M., Kendall, C., McGlynn, B. L., Welker, J. M., and Seibert, J.: The role of topography on catchment-scale water residence time: CATCHMENT-SCALE WATER RESIDENCE TIME, *Water Resour. Res.*, 41, <https://doi.org/10.1029/2004WR003657>, 2005.
- Meybeck, M., Green, P., and Vörösmarty, C.: A New Typology for Mountains and Other Relief Classes: An Application to Global Continental Water Resources and Population Distribution, *Mt. Res. Dev.*, 21, 34–
605 45, [https://doi.org/10.1659/0276-4741\(2001\)021\[0034:ANTFMA\]2.0.CO;2](https://doi.org/10.1659/0276-4741(2001)021[0034:ANTFMA]2.0.CO;2), 2001.
- Moon, S., Perron, J. T., Martel, S. J., Holbrook, W. S., and St. Clair, J.: A model of three-dimensional topographic stresses with implications for bedrock fractures, surface processes, and landscape evolution: Three-Dimensional Topographic Stress, *J. Geophys. Res. Earth Surf.*, 122, 823–846, <https://doi.org/10.1002/2016JF004155>, 2017.
- 610 Müller Schmied, H., Cáceres, D., Eisner, S., Flörke, M., Herbert, C., Niemann, C., Peiris, T. A., Popat, E., Portmann, F. T., Reinecke, R., Schumacher, M., Shadkam, S., Telteu, C.-E., Trautmann, T., and Döll, P.: The global water resources and use model WaterGAP v2.2d: Model description and evaluation, *Hydrology*, <https://doi.org/10.5194/gmd-2020-225>, 2020.
- Muñoz-Villers, L. E., Geissert, D. R., Holwerda, F., and McDonnell, J. J.: Factors influencing stream
615 baseflow transit times in tropical montane watersheds, *Hydrol. Earth Syst. Sci.*, 20, 1621–1635, <https://doi.org/10.5194/hess-20-1621-2016>, 2016.
- Napoli, A., Crespi, A., Ragone, F., Maugeri, M., and Pasquero, C.: Variability of orographic enhancement of precipitation in the Alpine region, *Sci. Rep.*, 9, 13352, <https://doi.org/10.1038/s41598-019-49974-5>, 2019.
- 620 Ponton, C., West, A. J., Feakins, S. J., and Galy, V.: Leaf wax biomarkers in transit record river catchment composition, *Geophys. Res. Lett.*, 41, 6420–6427, <https://doi.org/10.1002/2014GL061328>, 2014.
- Rempe, D. M. and Dietrich, W. E.: Direct observations of rock moisture, a hidden component of the hydrologic cycle, *Proc. Natl. Acad. Sci.*, 115, 2664–2669, <https://doi.org/10.1073/pnas.1800141115>, 2018.
- Roe, G. H. and Baker, M. B.: Microphysical and Geometrical Controls on the Pattern of Orographic
625 Precipitation, *J. Atmospheric Sci.*, 63, 861–880, <https://doi.org/10.1175/JAS3619.1>, 2006.
- Scanlon, B. R., Zhang, Z., Save, H., Sun, A. Y., Müller Schmied, H., van Beek, L. P. H., Wiese, D. N., Wada, Y., Long, D., Reedy, R. C., Longuevergne, L., Döll, P., and Bierkens, M. F. P.: Global models underestimate large decadal declining and rising water storage trends relative to GRACE satellite data, *Proc. Natl. Acad. Sci.*, 115, <https://doi.org/10.1073/pnas.1704665115>, 2018.
- 630 Stockinger, M. P., Bogen, H. R., Lücke, A., Diekkrüger, B., Cornelissen, T., and Vereecken, H.: Tracer sampling frequency influences estimates of young water fraction and streamwater transit time distribution, *J. Hydrol.*, 541, 952–964, <https://doi.org/10.1016/j.jhydrol.2016.08.007>, 2016.
- Tang, W. and Carey, S. K.: HydRun: A MATLAB toolbox for rainfall-runoff analysis, *Hydrol. Process.*, 31, 2670–2682, <https://doi.org/10.1002/hyp.11185>, 2017.



635 Tetzlaff, D., Seibert, J., McGuire, K. J., Laudon, H., Burns, D. A., Dunn, S. M., and Soulsby, C.: How does landscape structure influence catchment transit time across different geomorphic provinces?, *Hydrol. Process.*, 23, 945–953, <https://doi.org/10.1002/hyp.7240>, 2009a.

Tetzlaff, D., Seibert, J., and Soulsby, C.: Inter-catchment comparison to assess the influence of topography and soils on catchment transit times in a geomorphic province; the Cairngorm mountains, Scotland, *Hydrol. Process.*, 23, 1874–1886, <https://doi.org/10.1002/hyp.7318>, 2009b.

640 Torres, M. A., West, A. J., Clark, K. E., Paris, G., Bouchez, J., Ponton, C., Feakins, S. J., Galy, V., and Adkins, J. F.: The acid and alkalinity budgets of weathering in the Andes–Amazon system: Insights into the erosional control of global biogeochemical cycles, *Earth Planet. Sci. Lett.*, 450, 381–391, <https://doi.org/10.1016/j.epsl.2016.06.012>, 2016.

645 Tucker, G. E. and Bras, R. L.: A stochastic approach to modeling the role of rainfall variability in drainage basin evolution, *Water Resour. Res.*, 36, 1953–1964, <https://doi.org/10.1029/2000WR900065>, 2000.

Viviroli, D., Dürr, H. H., Messerli, B., Meybeck, M., and Weingartner, R.: Mountains of the world, water towers for humanity: Typology, mapping, and global significance: MOUNTAINS AS WATER TOWERS FOR HUMANITY, *Water Resour. Res.*, 43, <https://doi.org/10.1029/2006WR005653>, 2007.

650 West, A., Galy, A., and Bickle, M.: Tectonic and climatic controls on silicate weathering, *Earth Planet. Sci. Lett.*, 235, 211–228, <https://doi.org/10.1016/j.epsl.2005.03.020>, 2005.

Wilusz, D. C., Harman, C. J., and Ball, W. P.: Sensitivity of Catchment Transit Times to Rainfall Variability Under Present and Future Climates, *Water Resour. Res.*, 53, 10231–10256, <https://doi.org/10.1002/2017WR020894>, 2017.

655

660

665